ISOCAM 3-12 μm IMAGING OF FIVE GALACTIC COMPACT H II REGIONS

A. Zavagno

Institut d'Astrophysique de Marseille, 2 Place Le Verrier, 13248 Marseille Cedex 4, France

Abstract

ISOCAM 3-12 μm imaging of five Galactic compact H II regions reveals the spatial distribution of the unidentified infrared band (UIB) emission and underlying continua. The derived UIB intensities (continuum subtracted) agree well with those found from previous works. The distribution of the UIB emission is similar in the five regions: the UIB emission peaks just outside the ionisation front, in the photodissociation region (PDR). Moreover, in four of the five sources for which data exist, the UIB emission zones correlates well with those of 2.12 μm H_2 emission due to fluorescence. UIB emission seems to be related to the molecular and/or atomic hydrogen but this link remains unclear. The 12 μm CVF emission observed with ISOCAM shows a peak near the exciting star in high excitation regions. This indicates that the very small grains, responsible for the strong rising continuum observed in compact H II regions, are located near the star. The (LW6/LW9) ratio obtained using ISOGAL images confirms this result. This ratio can be used as an indicator of the relative importance of the UIB carriers to the very small grains. The high (LW6/LW9) value (2–3) observed in the PDR confirms that the UIB carriers are concentrated there.

The perspectives using FIRST are presented.

Key words: ISM: Dust – ISM: H II regions – ISM: lines and bands

1. Introduction

A serie of infrared emission bands is observed in various astrophysical environments between 3 and 12 μm. Duley & Williams (1981) were the first to note that some UIB wavelengths are characteristic of the bending and streching modes of CC and CH bonds in aromatic molecules. Since then, various carriers have been proposed for these bands including the polycyclic aromatic hydrocarbons (PAHs; Léger & Puget 1984, Allamandola et al. 1985) and more amorphous materials containing aromatic hydrocarbons (Sakata et al. 1984, Borghesi et al. 1987, Papoular et al. 1989). However, despite a large number of theoretical and laboratory studies, the carriers of these bands are still a matter of debate. Various problems remain with the proposed species. The observation of UIB emission in UV-poor environments (Uchida et al. 1998, Pagani et al. 1999, Uchida et al. 2000) poses the problem of the excitation mechanism that is assumed, for PAH molecules, to be the absorption of a UV photon. Another problem is the stability of the UIB spectrum (band positions and profiles) in very different UV environments. Indeed, theoretical and laboratory works on PAHs predict important changes in the UIB spectra (band intensity ratios) as a function of the UV radiation field, changes that are not observed (Uchida et al. 2000). In order to study the impact of the physical environment (UV field, gas density) on the UIB emission, we observed five Galactic compact H II regions between 3 and 12 μm with ISOCAM (Cesarsky et al. 1996). Section 1 presents the sample and the data reduction. Results are given in Section 2. The conclusions and perspectives of this work using the FIRST satellite are drawn in Section 4.

2. Observations

Sh 61, Sh 138, Sh 152, Sh 156, Sh 186 (Sharpless 1959) have been observed with ISOCAM. These sources were selected on the basis of their high 12 μm brightness (IRAS 12 μm flux $\geq$ 10 Jy), the presence of the UIBs together with the absence of silicate absorption at 10 and 18 μm on their IRAS/LRS spectra and their small (diameter $\leq 3'$) optical size. The knowledge of the spectral type for the main exciting star was also required. The source properties are summarised in Table 1. Due to limited space, only the results obtained for Sh 156 will be presented here. Results for the whole sample together with references for the quantities in Table 1 are given in Zavagno & Ducci (2001). Columns 1 and 2 give the names of the sources and of the associated IRAS sources. The spectral type of the main exciting star is given in column 3. The distance is given in column 4. The total luminosity taken from Vacca et al. (1996) for the given spectral type is given in column 5. The 91–245 nm luminosity is given in column 6. This luminosity (noted $L_{\rm UV}$ in Table 1) is derived from the stellar models of Schaerer & de Koter (1997) assuming the given spectral type. Note that these two luminosity values represent lower limits, as the main exciting star is often found associated with a dense cluster in such regions (Deharveng et al. 1999, Smutko & Larkin 1999). The UV luminosity is needed to better characterize the UIB emission as a func-

Proc. Symposium *'The Promise of the Herschel Space Observatory'* 12–15 December 2000, Toledo, Spain
ESA SP-460, July 2001, eds. G.L. Pilbratt, J. Cernicharo, A.M. Heras, T. Prusti, & R. Harris

tion of the UV radiation field.

Table 1. Main properties of the observed sources

Source	IRAS Name	ST	Distance kpc	$\log L_{\rm TOT}$ $L_\odot$	$\log L_{\rm UV}$ $L_\odot$
Sh 61	18306−0500	B0e	2.5	4.881	4.666
Sh 138	22308+5812	O9V	5	5.061	4.75
Sh 152	22566+5830	O9V	3.6	5.061	4.75
Sh 156	23030+5958	O7V	5.75	5.404	4.94
Sh 186	01056+6251	O9.5V	3.6	4.972	4.70

The pixel size was $3''$ and the small field mirror was used. Figure 1 presents the R-band image of Sh 156 extracted from the Digitized Sky Survey (DSS-II). The field observed with ISOCAM is shown (black box). The 6cm-radio emission (Birkinshaw 1978) has been superimposed on the optical image (white contours). The field covered by ISO-

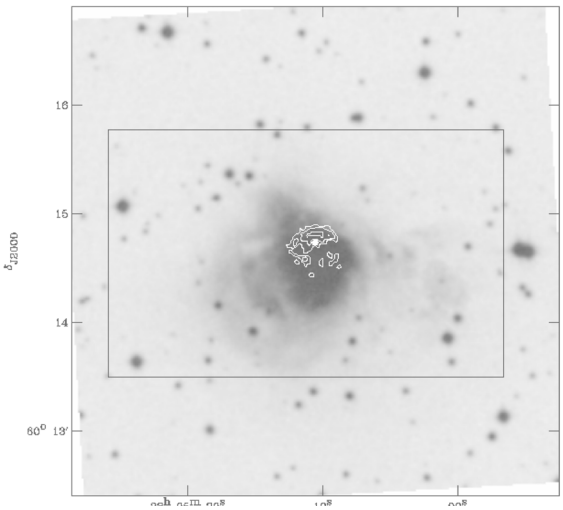

Figure 1. DSS R-band image and ISOCAM field (black box) for Sh 156. Radio emission is superimposed (white contours). The white dot represents the position of the main exciting star. North is up, east is left

CAM for Sh 156 is $174''\times87''$. Observations using the SW1 (3.05–4.1 μm), SW2 (3.2–3.4 μm), LW4 (5.5–6.5 μm), LW6 (7–8.5 μm) and LW8 (10.7–12 μm) filters were obtained to look at the distributions of the 3.3, 6.2, 7.7 and 11.2 μm emission bands and the underlying continuum. Five CVF observations were made at 5.985, 6.911, 8.222, 10.520 and 12.000 μm with a FWHM that varies between 0.156 and 0.295 μm. Figure 2 presents two parts of the ISO-SWS spectrum of Sh 156, from 3 to 4.15 μm and from 5 to 13 μm. The ISOCAM filters and CVF positions are shown.

The data were processed using CAM Interactive Analysis (CIA, Ott et al. 1997). The standard procedure was applied: dark correction, deglitching, stabilisation, flat field

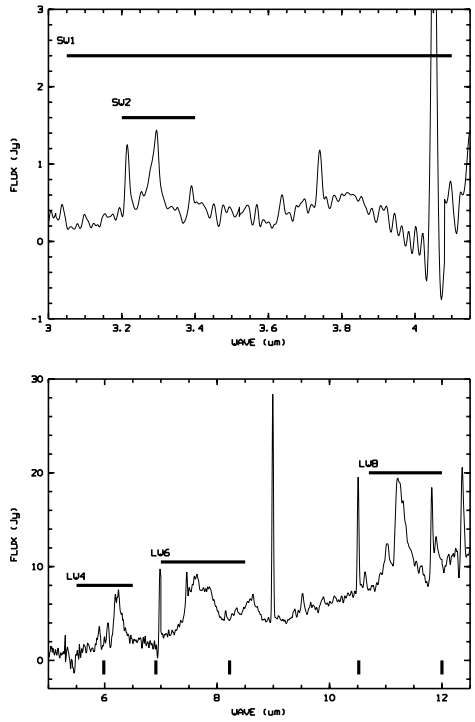

Figure 2. ISO-SWS spectrum of Sh 156 from 3 to 4.15 μm (top) and from 5 to 12.5 μm (bottom). The ISOCAM filters and CVF positions are shown

correction and calibration (Stark et al. 1999 for details). Transient correction has been applied to CAM-SW and CAM-LW data (Tiphène et al. 2000 and Coulay & Abergel 1999).

3. Results

3.1. Observed emissions

As shown in Fig. 2 the ISOCAM filters cover the main UIBs at 3.3 (SW2), 6.2 (LW4), 7.7 (LW6) and 11.3 μm (LW8). The CVF measurements, when not affected by ionic line emission, are used to estimate the underlying continuum for these bands. The continuum associated with the 3.3 μm band was estimated from the SW1 emission.

Little or no UIB emission (continuum subtracted) is observed in the ionized zone. This indicates the possible destruction of the carriers in strong radiation fields and/or the non-efficency of the excitation mechanism (Onaka et al. 2000). The radiation pressure can also sweep-up the UIB carriers outside the ionized region, increasing the dust-to-gas ratio in the photodissociation region (Weingartner & Draine 1999). Another case of such a distribution is observed in Sh 88 where the dust emission, observed with ISOCAM in the 5–8 μm range, is concentrated in a shell that surrounds the ionized zone (Deharveng et al. 2000).

3.2. The 6.2 μm band distribution

As seen in Fig. 2, the 5.9 μm CVF measurement can be used to remove the continuum of the 6.2 μm band observed with the LW4 filter. The distribution of the 6.2 μm band emission (continuum subtracted) is shown in Figure 3, superimposed (contours) on a map of the strong 2.12 μm H_2 emission due to fluorescence (see Smutko & Larkin 1999). The two emissions spatially coincide, as for the three other

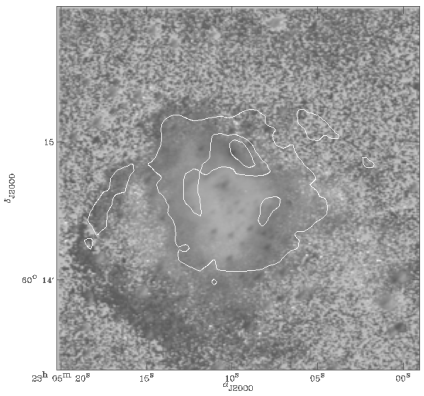

Figure 3. Zone of strong 2.12 μm emission of H_2 (black zones) due to fluorescence together with contours of the 6.2 μm band emission (continuum subtracted)

H II regions (Sh 61, Sh 152, Sh 186) for which near infrared H_2 data exist (Smutko & Larkin 1999). This correlation between UIB and 2.12 μm emissions is observed for strong and low UIB emission in the ISOCAM sample and has also been observed towards the edge of the Rho Ophiucus main cloud (Habbart et al. 2000). In NGC 7023, the UIB intensities are linked to the density of atomic hydrogen (Tran 1998). UIB emission seems to be related to the hydrogen emission but this link remains unclear. Papoular (2000) has proposed an excitation mechanism, the chemiluminescence, based on the excitation of the vibrations of the chemical bonds of carbonaceous dust by impact of gaseous H atoms. Mennella et al. (2000) show that the 3.4 μm band can be activated in carbon grains by exposure to atomic hydrogen. Hydrogen could then explain the presence of UIB emission in UV-poor environments and the enhancement of UIB emission in dense H I–H_2 zones. Understanding the link between hydrogen and UIB emissions is the next step in this research field.

3.3. The UIB and 12 μm emissions

The CVF 12 μm emission is presented in Figure 4. In Sh 156, this emission peaks around the star and then follows well that of the UIBs. In Sh 138, Sh 152 and

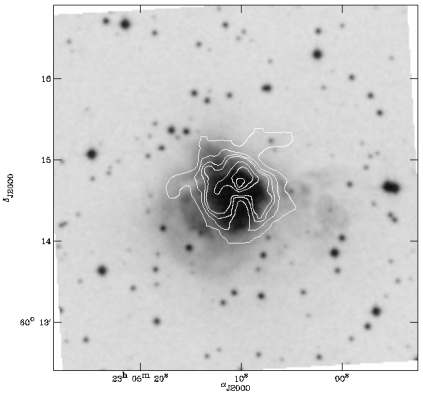

Figure 4. ISOCAM CVF 12 μm emission of Sh 156 (contours) superimposed on an R-band image of the region

Sh 186, regions of lower excitation degree, no peak of the 12 μm emission is observed near the star. Very small grains (VSGs, Désert et al. 1990) are believed to be responsible for the strong rising continuum observed in compact H II regions (Roelfsema et al. 1998). The SWS and LWS spectra of Sh 138 show that the contribution of this grains' population to the 6–12 μm continuum is low. This is not the case for Sh 156. The peak of the 12 μm emission near the star in highly excited regions indicates that the VSGs survive in hard radiation fields.

3.4. Distribution of the (LW6/LW9) emission

The LW9 filter (14–16 μm) covers part of the strong rising continuum observed in many H II regions observed with ISO (Roelfsema et al. 1998). As seen in Fig. 2, the LW6 filter contains the 7.7 (and part of the 8.6 μm) band. The (LW6/LW9) ratio is then an indicator of the relative importance of the UIB carriers to the very small grains. Using the ISOGAL (Omont et al. 1999) images, I derived this ratio for Sh 138, Sh 152 and Sh 156. The result obtained for Sh 156 is shown in Figure 5. The bright (LW6/LW9) zones coincides well with zones of bright 2.12 μm H_2 emission (see Fig. 3). In Sh 138, Sh 152 and Sh 156, similar (LW6/LW9) values are observed at different distance from the main exciting star. A model of the available radiation field is needed to interpret these values in terms of grain abundance variations. A low (LW6/LW9) value is observed near the star in Sh 156, due to the presence of the [NeIII] line at 15.5 μm. Because Ne^{++} has a high ionisation potentiel (40.963 eV) the (LW6/LW9) ratio can also be an ionisation indicator in compact H II regions. Caution has to be taken for highly embedded objects, due to the presence of CO_2 ice absorption feature at 15 μm (Roelfsema et al. 1998) but this is not the case for the three regions considered here.

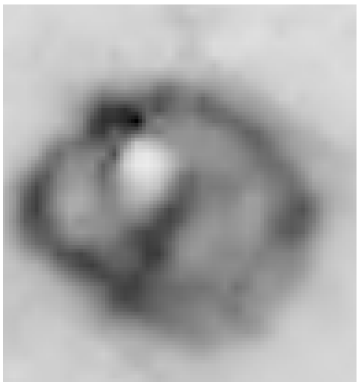

Figure 5. Zoom of the (LW6/LW9) ratio using the ISOGAL images (see text). The "background" value is 0.55, the value near the star is 0.2 and the maximum value is 3. The white zone at the centre corresponds to the ionized region

4. Conclusions and perspectives

The UIBs are present and show comparable properties in the five observed regions with emission peaks that are always found in the PDRs. The distribution of the 6.2 μm band and of the (LW6/LW9) ratio coincide well with that of the 2.12 μm H_2 emission. The UIB emission seems to be related to the hydrogen (atomic and/or molecular) but the possible link between the UIB emission and hydrogen remains unclear.

The FIRST satellite offers several perspectives, like the possibility to study the link between the small and large dust grains. Imaging of compact H II regions at 350 μm with a 11″ spatial resolution has recently been obtained at the CSO (Hunter et al. 2000). Results on Sh 138 show that the cold dust emission is concentrated to the south of the optical ionized region, towards the molecular cloud. UIB emission is also observed in this direction. The PACS instrument will offer a high sensitivity together with a high spatial resolution, comparable to ISOCAM (3–6″). In particular, the bolometer wavelength range (60–210 μm) is well suited to study the relation between the different dust grain populations. Another point is to better characterize the PDRs (density, temperature) in these regions. Indeed, because the main UIB emission takes place in this zone, a good knowledge of the physical conditions is needed if one wants to constrain the nature of the UIB carriers, through the determination of the excitation conditions, for example. FIRST/PACS and HIFI are well suited to this purpose, allowing to obtain complete line surveys of those PDRs. On larger scales, the systematic search for embedded massive stars near compact H II regions will be possible. Triggered star formation is believed to be an important process in OB associations (Elmegreen & Lada 1977) due to the propagation of the ionisation front in the molecular cloud. No systematic study has been done until now, due to the poor sensitivity and spatial resolution in the far-IR and submillimetre ranges. The existence of multiwavelength databases, especially in the near-IR (2MASS, DENIS) and mid-IR ranges, will be very usefull to select the candidates that will be observed with FIRST. A good example of this is the Sh 152–Sh 153 region seen with ISOGAL (Copet & Zavagno 1999).

References

Allamandola L.J., Tielens A.G.M.M, Barker J.R., 1985, ApJ 290, L25

Birkinshaw M., 1978, MNRAS 182, 401

Borghesi A., Bussoletti E., Colangeli L., 1987, ApJ 314, 422

Cesarsky C.J., Abergel A., Agnèse P. et al., 1996a, A&A 315, L32

Copet E., Zavagno A., 1999, ESA-SP 427, 659

Coulais A., Abergel A., 1998, in 'The Universe as seen by ISO', ESA publications, SP-427, 61, Cox P., Kessler M. eds

Deharveng L., Zavagno A., Nadeau D., Caplan J., Petit M., 1999, A&A 344, 943

Deharveng L., Nadeau D., Zavagno A., Caplan J., 2000, A&A 360, 1107

Désert F.X., Boulanger F., Puget J.-L., 1990, A&A 237, 215

Duley W. W. & Williams D.A., 1981, MNRAS 196, 269

Elmegreen B., Lada C., 1977, ApJ 214, 725

Habart E., Boulanger F., Verstraete L., Falgarone E., Pineau des Forets G., Abergel A., 2000, ESA SP-456, in press

Hunter T.R., Churchwell E., Watson C., Cox P., Benford D.J., Roelfsema P.R., 2000, ApJ 119, 2711

Léger A., Puget J.-L., 1984, A&A 137, L5

Mennella V., Brucato J.R., Colangeli L., 1999, ApJ 524, L71

Omont A. and the ISOGAL team, 1999, ESA SP-427, 211

Onaka T., Mizutani M., Chan K.-W., Tomono D., Shibai H., Nakagawa T., Doi Y., 2000, ESA-SP 456, in press

Ott S., Abergel A., Altieri B., Augueres J-L., Aussel H., et al., 1997, ASP Conf. Series 125, 34

Pagani L., Lequeux J., Cesarsky D., Donas J., Millard B., Loinard L., Sauvage M., 1999, A&A 351, 447

Papoular R., Conard J., Guiliano M., Kister J., Mille G., 1989, A&A 217, 204

Papoular R., 2000, A&A 359, 397

Roelfsema P.R., Cox P., Kessler M., Baluteau J.-P., 1998, ASP Conf. Series 132, 76

Sakata A., Wada S., Tanabe T., Onaka T., 1984, ApJ 287, L51

Schaerer D., de Koter A., 1997, A&A 322, 598

Sharpless S., 1959, ApJS 4, 257

Smutko M.F., Larkin J.E., 1999, AJ 117, 2448

Stark J.-L., Abergel A., Aussel H., Sauvage M., Gastaud R., Claret A., Desert X., Delattre C., Pantin E., 1999, A&A Suppl. Ser. 134, 135

Tiphène D., Rouan D., Epstein G., Le Coupanec P., 2000, Experimental Astronomy, 10 (Issue 2/3), 347

Tran Q.D., 1998, Thèse, Université Paris XI

Uchida K.I., Sellgren K., Werner M., 1998, ApJ 493, L109

Uchida K.I., Sellgren K., Werner M., Houdashelt M.L., 2000, ApJ 530, 817

Vacca W.D., Garmany C.D., Shull J.M., 1996, ApJ 460, 914

Weingartner J.C., Draine B.T., 1999, ESA SP-427, 783

Zavagno A., Ducci V., 2001, A&A submitted